Gating Properties of Heterotypic Gap Junction Channels Formed of Connexins 40, 43, and 45

Mindaugas Rackauskas,* Maria M. Kreuzberg,‡ Mindaugas Pranevicius,† Klaus Willecke,‡ Vytas K. Verselis,* and Feliksas F. Bukauskas*

*Department of Neuroscience and †Department of Anesthesiology of Albert Einstein College of Medicine, Bronx, New York; and ‡Institut für Genetik, Abteilung Molekulargenetik, Universität Bonn, Bonn, Germany

ABSTRACT Connexins (Cxs) 40, 43, and 45 are expressed in many different tissues, but most abundantly in the heart, blood vessels, and the nervous system. We examined formation and gating properties of heterotypic gap junction (GJ) channels assembled between cells expressing wild-type Cx40, Cx43, or Cx45 and their fusion forms tagged with color variants of green fluorescent protein. We show that these Cxs, with exception of Cxs 40 and 43, are compatible to form functional heterotypic GJ channels. Cx40 and Cx43 hemichannels are unable or effectively impaired in their ability to dock and/or assemble into junctional plaques. When cells expressing Cx45 contacted those expressing Cx40 or Cx43 they readily formed junctional plaques with cell-cell coupling characterized by asymmetric junctional conductance dependence on transjunctional voltage, V_j. Cx40/Cx45 heterotypic GJ channels preferentially exhibit V_j-dependent gating transitions between open and residual states with a conductance of ~42 pS; transitions between fully open and closed states with conductance of ~52 pS in magnitude occur at substantially lower (~10-fold) frequency. Cx40/Cx45 junctions demonstrate electrical signal transfer asymmetry that can be modulated between unidirectional and bidirectional by small changes in the difference between holding potentials of the coupled cells. Furthermore, both fast and slow gating mechanisms of Cx40 exhibit a negative gating polarity.

INTRODUCTION

Connexins (Cxs), a large family of homologous membrane proteins, form gap junction (GJ) channels that provide a direct pathway for electrical and metabolic signaling between cells (1,2). Each GJ channel is composed of two hemichannels (connexons), which in turn are composed of six Cx subunits. Thus far, at least 20 distinct Cx isoforms have been cloned (3). Cell-cell communication can be organized through homotypic (same Cx isotype in both hemichannels), heterotypic (hemichannels differ in Cx isotypes) or/and heteromeric (different Cx isotypes in at least one hemichannel) channels that vary highly in conductance, perm-selectivity, and gating properties (2).

Cx40, Cx43, and Cx45 are expressed in different tissues, but most abundantly in cardiovascular and central nervous systems. Cx40, Cx43, and Cx45 have been regarded as the three major cardiac connexins (3,4). mCx30.2 has been recently identified as the fourth cardiac connexin in rodents; its putative human ortholog is Cx31.9 (5). Given the specific expression patterns of these connexins, their capacity to form heterotypic and heteromeric junctions will significantly influence the nature of intercellular communication and the spread of excitation within and between different regions of the heart (6–9). Blood vessels express Cx40, Cx43, Cx45, and Cx37, with Cx40 most abundantly expressed in endothelial cells and Cx43 in smooth muscle cells (10). In the CNS, astrocytes abundantly express Cx43, endothelial cells of the blood-brain barrier express Cx40 and Cx43 (11), and neurons of the olivocerebellar system express Cx45 (12). Accordingly, a number of studies have reported malformation and dysfunction not only of the heart, but also of the whole cardiovascular system of mice in which Cx40, Cx43, or Cx45 were knocked out (13–16). Only Cx40 knockout mice survive during the postnatal period and they exhibit severe dysfunction of the cardiovascular system, such as impaired sinoatrial-nodal function, slowed conduction velocity in atria and the AV node, impaired conduction in bundle branches, structural abnormalities of endothelial and smooth muscle layers in the blood vessels, deficient conduction of vasodilator stimuli along vessel walls, elevated mean arterial pressure and blood pressure regulation abnormalities (17–20).

Several studies reported formation of functional heterotypic junctions between cells expressing Cx45 with those expressing Cx40 and Cx43 (21–25). Initial electrophysiological studies in *Xenopus* oocytes (10) and HeLa transfectants (26) reported that Cx40 and Cx43 do not form functional heterotypic channels. These findings were confirmed subsequently in pairs of *Xenopus* oocytes expressing Cx40 and Cx43 (27). Furthermore, when HeLa cells expressing Cx43 were cocultured with those expressing Cx40, immunohistochemical evidence for formation of heterotypic junctional plaques (JPs) was lacking (26) suggesting that Cx40 and Cx43 hemichannels are unable to dock or to cluster into visible JPs. Those studies were stimulated by findings that Cx40 and Cx43 are expressed in different cell types in the cardiovascular system that come into direct contact. Cx43 is the major connexin expressed in working myocardium of the heart and smooth muscle cells of the blood vessels,

Submitted October 11, 2006, and accepted for publication December 4, 2006.

Address reprint requests to Dr. Feliksas F. Bukauskas, 1300 Morris Park Ave., Albert Einstein College of Medicine, Bronx, NY 10461. Tel.: 718-430-4130; Fax: 718-430-8944; E-mail: fbukausk@aecom.yu.edu.

0006-3495/07/03/1952/14 $2.00

doi: 10.1529/biophysj.106.099358

whereas Cx40 is mainly expressed in the atrium, atrioventricular node, AV bundle, and endothelial cells. These findings suggested that intercellular communication can be spatially regulated by the selective expression of different connexins. An inability to form heterotypic junctions would preclude communication between cells residing in close apposition, perhaps enabling them to perform different function, e.g., endothelial and smooth muscle cells or cells of the conduction system and working myocardium of the heart. Subsequent electrophysiological studies in transfected mammalian cells reported that Cx40 and Cx43 can form functional heterotypic channels although junctional conductance was low (21–23). More recently, concerns have been raised that the reported coupling between Cx40- and Cx43-expressing cells may have been caused by formation of heterotypic/heteromeric junctions with an endogenous connexin rather than by Cx40/Cx43 heterotypic junctions (28) and low efficiency of formation of heteromeric junctions was reported due to inability of Cx40 and Cx43 to dock (29).

Here, we examined formation and gating properties of heterotypic junctions in HeLa cells stably transfected with Cx40, Cx43, or Cx45 in native and GFP-fused forms. We demonstrate that heterologous Cx40/Cx43 HeLa cell pairs lack JPs composed of Cx40 and Cx43 and exhibit low levels of coupling explained by the formation of heterotypic junctions with endogenously expressed Cx45, i.e., Cx40/Cx45 and Cx43/Cx45 junctions. We show that in response to transjunctional voltage (V_j), Cx40/Cx45 heterotypic GJ channels exhibit mainly gating transitions between the fully open state (~52 pS) and the residual state (~10 pS), giving rise to 42 pS gating transitions. The residual state of Cx45 hemichannels rectifies and we demonstrate signal transfer asymmetry in Cx40/Cx45 junctions that can be modulated from unidirectional to bidirectional by small changes in the difference of the holding potentials of coupled cells. We show that both fast and slow gates of Cx40 exhibit a negative gating polarity.

METHODS

Cell lines and culture conditions

Experiments were performed on HeLa cells (a human cervix carcinoma cell line, ATCC No. CCL-2) transfected with wild-type Cx40, Cx43, or Cx45 and their fusion forms with color variants of green fluorescent protein (EGFP or CFP). HeLa cells were stably transfected with cDNAs encoding wild-type rat Cx43 or Cx43-EGFP, wild-type mouse Cx40 or Cx40-CFP and wild-type mouse Cx45. HeLa cells were grown in Dulbecco's medium supplemented with 10% FBS. All media and culture reagents were obtained from Life Technologies (GIBCO BRL). The transfection procedure has been described previously (5,30). To study heterotypic junctions, two types of cells expressing different connexins were mixed in equal quantities and seeded at a density of $\sim 10^4$ cells/cm^2 on coverslips placed in culture dishes.

Electrophysiological measurements

For simultaneous electrophysiological and fluorescence recording, cells were grown on 22 × 22 mm No. 0 coverslips and transferred to an experimental chamber (31) mounted on the stage of Olympus IX70 inverted microscope (Olympus America, Melville, NY) equipped with a fluorescence imaging system. The chamber was perfused with a modified Krebs-Ringer solution containing (in mM): 140 NaCl, 4 KCl, 2 $CaCl_2$, 1 $MgCl_2$, 5 HEPES, 5 glucose, 2 pyruvate (pH = 7.4). Patch pipettes were filled with pipette solution containing (in mM): 10 Na Asparpate, 130 KCl, 0.26 $CaCl_2$, 1 $MgCl_2$, 3 MgATP, 5 HEPES (pH 7.2), 2 EGTA ($[Ca^{2+}] = \sim 5 \times 10^{-8}$ M).

Junctional conductance, g_j, was measured using the dual whole-cell patch clamp system (32,33). Briefly, each cell of a pair was voltage clamped to the same holding potential ($V_1 = V_2$) with a separate patch clamp amplifiers. By stepping the voltage in one cell and keeping the other constant (V_2), junctional current (I_j) was measured as the change in current in the unstepped cell, I_2, in response to the applied transjunctional voltage ($V_j = V_2 - V_1$). We generally maintained the holding potential in the unstepped cell close to the resting potential to reduce the noise in I_j that is generated by nonjunctional current. Thus, g_j is obtained by dividing the change in I_2 by V_j. With low levels of coupling, unitary junctional currents can be recorded as discrete quantal changes in the unstepped cell that are accompanied by equal and opposite quantal changes in the stepped cell. Voltages and currents were digitized using a MIO-16× A/D converter (National Instruments, Austin, TX) and acquired and analyzed using custom-made software designed by E. B. Trexler and V. K. Verselis.

In all cocultures of cells expressing different combinations of Cx isoforms at least one type of cell expressed a Cx fused with GFP to allow visualization of Cx distribution, particularly the size and number of junctional plaques. All cell lines expressing wild-type Cxs before coculturing were prelabeled with DAPI or DiI (Invitrogen, Carlsbad, California). Isolated heterotypic pairs were selected by identifying pairs of cells in which cells were expressing GFPs of different color or one expressed GFP and the other was labeled with DAPI or DiI. Isolated heterologous pairs were selected for recording between 24 and 60 h after platting.

Fluorescence imaging

Fluorescence images were acquired and analyzed using a Hamamatsu cooled digital camera mounted on an Olympus IX70 microscope and UltraVIEW software for image acquisition and analysis (PerkinElmer Life Sciences, Boston, MA). Appropriate excitation and emission filters (Chroma Technology, Brattleboro, VT) were used to image CFP, EGFP, DAPI, and DiI.

RESULTS

Fluorescence imaging and electrophysiology of Cx40 and Cx43 heterologous cell pairs

We examined whether there was evidence of Cx40/Cx43 heterotypic junction formation using several different types of heterologous cell pairings. In all heterologous pairing combinations examined, at least one cell type expressed a GFP-tagged form to allow visualization of JPs. Fig. 1 *A* illustrates a group of HeLa cells expressing either Cx40-CFP (shown in *cyan*) or Cx43-EGFP (shown in *red*). The images show that homotypic JPs readily form, evident as large CFP or EGFP fluorescing puncta in regions of contacting Cx40-CFP and Cx43-EGFP cells, respectively. For more details, see Movie 1 in the Supplementary Material, which shows the absence of JPs between cells expressing Cx40-CFP (in *green*) and Cx43-EGFP (in *red*), whereas large JPs are visible between cells that both express Cx40-CFP or Cx43-EGFP. Typically, GFP fluorescence associated with JPs is significantly stronger than the fluorescence of connexin protein

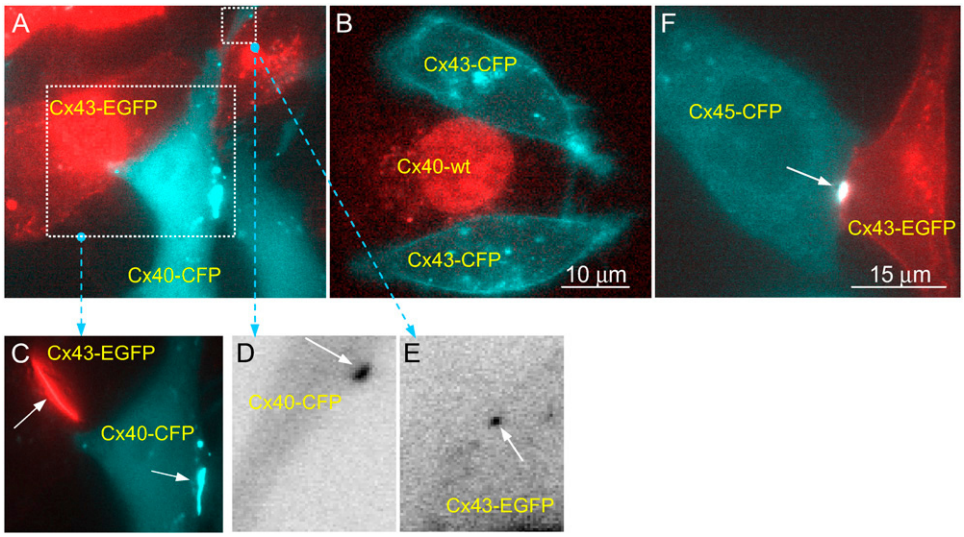

FIGURE 1 Absence of Cx40/Cx43 junctional plaque formation in HeLa cells. (*A*) A cluster of HeLaCx40-CFP (*cyan*) and HeLaCx43-EGFP (*red*) cells exhibiting large junctional plaques formed of Cx40-CFP and Cx43-EGFP homotypic junctions; all in pseudocolors. In *C* is shown the inset from image (*A*) at lower fluorescence intensity to better visualize the junctional plaques (see *arrows*). (*B*) A cluster of two HeLaCx43-CFP cells (*cyan*) and a HeLaCx40-wt cell labeled with DAPI (*red*). (*D–E*) Fluorescence images in negative conversion from the region of interest indicated by the square in (*A*). Images of Cx40-CFP (*D*) and Cx43-CFP (*E*) from the same region of interest illustrate that small junctional plaques (shown by *arrows*) form but do not overlap. (*F*) Color overlap of a cell pair formed of HelaCx43-EGFP (red) and HeLaCx45-CFP (*cyan*) cells. The arrow points to the junctional plaque.

residing intracellularly or in the nonjunctional plasma membrane. This intense fluorescence of JPs is evident in Fig. 1 *C* where the image from a region of interest (indicated by the *square* in Fig. 1 *A*) containing JPs is shown at substantially reduced intensity of emitted light (see *white arrows*). No such large JPs were evident between contacting Cx40-CFP and Cx43-EGFP cells. Fig. 1 *B* shows a Cx40 cell labeled with DAPI (shown in *red*) in contact with two Cx43-CFP cells. Neither of the Cx43-CFP cells shows clearly identifiable JPs with the contacting Cx40 cell. All together, we performed 35 experiments with fluorescence imaging and in each experiment we examined more than 20 heterologous cell pairs. We did not observe a single junctional plaque that showed overlap of Cx40-CFP and Cx43-EGFP fluorescence in >700 cell pairs.

Upon closer inspection of these same images in white-black conversion to improve contrast (Fig. 1, *D* and *E*), small fluorescent puncta were occasionally visible at regions of contact between Cx40- and Cx43-expressing HeLa cells (*white arrows* in Fig. 1, *D* and *E*). We ascribe these small puncta to JPs because when imaged over time, they, like clearly identifiable JPs, were fixed in their movements to the plasma membrane visible by the distribution of labeled hemichannels (connexons) as a fluorescent line, whereas small fluorescent puncta typically representing cytosolic vesicles move randomly and independently of the movement of the plasma membrane. Images D and E are from the same region of interest but for CFP and EGFP fluorescence, respectively. The junctional puncta contain either CFP or EGFP fluorescence, but not both. Thus, these puncta cannot be Cx40-CFP/Cx43-EGFP heterotypic JPs, which would show colocalization of CFP and EGFP, and most probably represent Cx40-CFP/Cx45 and Cx43-EGFP/Cx45 heterotypic junctions as low levels of Cx45 expression in HeLa parental cells has been reported immunohistochemically (34). Double immunogold labeling of HeLa parental cells and HeLa transfectants expressing Cx40 and Cx43 also shows dispersed expression of GJ channel like particles formed of Cx45 (35). This finding correlates with electrophysiological data showing that among 29 HeLa parental cell pairs only three were coupled with an average g_j of 0.04 nS (21).

Fig. 1 *F*, which is pseudocolor overlap of EGFP (*red*) and CFP (*cyan*) signals, shows a junctional plaque in the region of contact between cells expressing Cx43-EGFP and Cx45-CFP. This cell pair exhibited electrical coupling with g_j = 17 nS. Similarly, we have observed junctional plaques between cells expressing Cx40 and Cx45 (not shown).

Electrophysiological examination of heterologous Cx40/Cx43 cell pairs showed that a majority were coupled, but that coupling was typically weak with mean g_j values for heterologous Cx40-CFP/Cx43-EGFP and Cx40/Cx43-EGFP combinations of 0.95 ± 0.59 nS (n = 25) and 1.06 ± 0.81 nS (n = 10), respectively. Only three cell pairs lacked coupling. All functionally coupled cell pairs exhibited gating asymmetry, which varied substantially among cell pairs. Examination of 35 homologous cell pairs formed of HeLa parental (untransfected) cells showed measurable coupling in only 5 cases, with g_j values in each case below 0.1 nS. When HeLa parental cells were paired with HeLa cells expressing either Cx40-CFP or Cx43-EGFP, all cell pairs were coupled, but g_j was low, ~0.3 and 0.5 nS, respectively. Thus, g_j measured between cells expressing Cx40 and Cx43 is close to the sum of g_js measured in Cx43/parental are Cx40/parental heterologous cell pairs, suggesting that heterotypic channels in which endogenous Cx45 pairs with Cx40 and Cx43 form in an independent fashion. The data obtained from different

pairing combinations are summarized in Table 1. These results indicate that coupling between HeLa parental cells is rare and low when it is present, likely because of low levels of Cx45 expression and consequently inefficient JP formation. Coupling and junction formation involving Cx45 remains low, but increases such that coupling levels of ~0.5 nS are achieved when at least one cell abundantly expresses Cx40 or Cx43.

Junctional conductance and voltage gating in heterologous cell pairs

In this series of experiments, we examined compatibility and gating properties of the three possible heterologous cell pair combinations than can be formed between cells expressing Cx40, Cx43, and Cx45.

Cx43 and Cx45

To examine compatibility between Cx43 and Cx45, we cocultured HeLa cells expressing Cx43-EGFP with those expressing Cx45 and found that JPs readily formed between heterologous cells, consistent with previous reports (24,25). We selected and examined heterologous cell pairs that contained at least one clearly identifiable and sizeable JP comprising a Cx43-EGFP/Cx45 heterotypic junction. Fig. 2 *A* shows the steady-state G_j-V_j dependence, which superimposes results of two types of measurements. Data points shown as open circles were collected from 24 Cx43-EGFP/Cx45 cell pairs by measuring g_j at the end of 30 s V_j steps. For each cell pair, g_j was normalized to its value at $V_j = 0$ to give normalized conductance, G_j. G_j-V_j dependence measured by applying long (150 s) V_j ramps (see *solid line*; averaged from three experiments) shows similar but slightly steeper G_j-V_j dependence for both V_j polarities; the difference suggests that steady-state may have been estimated better with the V_j ramps. As previously described in (25), albeit over a smaller range of V_j, Cx43-EGFP/Cx45 junctions exhibit a highly asymmetric steady-state G_j-V_j relation. G_j increases to a peak and decreases to near zero for modest

TABLE 1 Averaged g_js in different homo- and heterologous cell pairs

Junctions	Number of cell pairs	Conductance (g_j), nS
Cx40/Cx40	21	27.8 ± 7.1
Cx40/Cx40-CFP	36	23 ± 5.2
Cx40-CFP/Cx40-CFP	103	20.2 ± 2. 9
Cx40/Cx43-EGFP	10	1.06 ± 0.81
Cx40-CFP/Cx43-EGFP	25	0.96 ± 0.59
Cx40-CFP/Cx45	28	4.5 ± 3.1
Cx43-EGFP/Cx43-EGFP	45	28 ± 4
Cx43-EGFP/Cx45	35	13.3 ± 3.5
Cx40-CFP/HeLa parental	6	0.33 ± 0.27
Cx43-EGFP/HeLa parental	15	0.51 ± 0.25
HeLa parental/HeLa parental	35	Only in 5 $g_j > 0$

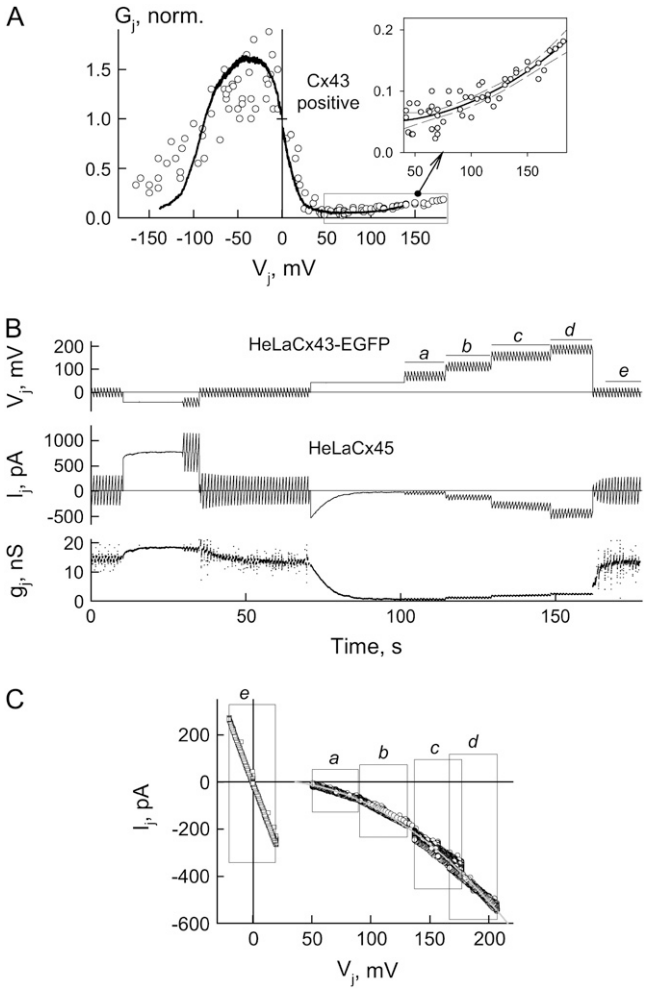

FIGURE 2 Voltage gating of Cx43/Cx45 heterotypic junctions. (*A*) Summary of G_j-V_j dependence of Cx45/Cx43-EGFP junctions; the data are shown as open circles and as a solid line were obtained by applying V_j steps and ramps, respectively, to one cell of a cell pair. The increase in G_j at an expanded scale is shown in the inset; dashed lines represent the confidence interval at $p = 95\%$. (*B*) Record of a junctional current (I_j) trace in response to voltage ramps and steps (*upper trace*) applied to the HeLaCx43-EGFP cell of a HeLaCx43-EGFP/Cx45 cell pair. Junctional conductance (g_j) was calculated as I_j/V_j. (*C*) I_j-V_j relationship measured by applying V_j ramps at different time intervals of the record (indicated by the *horizontal segments* labeled by letters *a-e*; on I_j-V_j plot the *squares* correspond to *segments* shown on the V_j *trace*). Open squares were recorded when holding potentials in both cells were equal, i.e., $V_j = 0$ mV. Open circles were recorded during the 100–160 s time period when voltage ramps were superimposed onto the V_j steps.

voltages relatively negative and positive, respectively, on the Cx43-EGFP side. This steep change in G_j has been shown to result from gating of the Cx45 hemichannel via its slow V_j gating mechanism (25). The reduction in G_j after reaching a peak for V_js relatively negative on the Cx43-EGFP side was shown to result from closure of the slow gate in Cx43-EGFP hemichannels, which is less steeply sensitive than in Cx45. The modest increase in G_j after a reduction to near zero for V_js relatively positive on the Cx43-EGFP side is ascribable

to an interaction between the slow and fast V_j gates that operate in series in Cx45 hemichannels (25). V_j acts on both gates, but closure of one gate would cause a larger fraction of V_j to drop across it thereby changing V_j across the other gate. In effect, the open probability of one gate is dependent on the state of the other, originally described by Harris et al. (36) to explain interaction between gates in separate hemichannels. The increasing conductance at large V_js can be explained by an increasing pool of Cx45 hemichannels entering the residual (subconductance) state (25).

To examine more closely this increase in g_j at large positive V_js and to determine whether it is caused, at least in part, by the rectification of the residual conductance of Cx45 hemichannel, we superimposed repeated V_j ramps of small amplitude onto large, long-lasting V_j steps (see Fig. 2 *B*). It was reported previously that the residual state of other connexins such as Cx32 and Cx43 possess a rectifying I/V relationship (37,38). Fig. 2 *B* shows an example of V_j and I_j records and the calculated g_j from a single Cx43-EGFP/Cx45 cell pair in which small (−20 to +20 mV) and brief (0.8 s) V_j ramps as well as long-duration V_j steps of different amplitudes were applied to the Cx43-EGFP cell. Initially, g_j was ~15 nS and increased ~20% in response to a negative V_j step of −40 mV. For a positive V_j step of +40 mV, g_j decreased rapidly to near zero, reaching steady state at g_j = ~0.7 nS. Stepwise increases in V_j (time interval, 100–160 s) resulted in an increase in g_j of nearly ~4-fold. All Cx43-EGFP/Cx45 cell pairs examined (mean $g_j = 13.3 \pm 3.5$ nS, $n = 35$) demonstrated this same behavior, which is atypical for most homotypic and heterotypic GJs, but is observed in Cx45 homotypic GJs (25) as well as in heterotypic junctions containing Cx45 on one side, such as Cx31/Cx45 (39) and Cx40/Cx45 (see below) junctions. This allowed us to compare I/V relations of channels that are largely in the open state to those that are gated to the residual state by V_j. Fig. 2 *C* shows superposed I/V plots measured during different time intervals when repeated ramps were superimposed onto V_j steps of different amplitudes (*a–d*) and during recovery from gating induced by these V_j steps (*e*); see corresponding lines and squares in Fig. 2, *B* and *C*, respectively. The I/V relationship measured in response to V_j ramps applied around $V_j = 0$ are essentially linear (see square *e*). In contrast, the I/V relationship measured in response to V_j ramps applied on top of V_j steps positive on the Cx43-EGFP side is nonlinear. Thus, both data sets shown in the inset of Fig. 2 *A* and in Fig. 2 *C* support the view that at positive V_js Cx45 hemichannels largely reside in the residual state, which rectifies. We conclude that it must be the Cx45 hemichannel that is gated to the residual substate as this form of gating in the Cx43-EGFP hemichannel is abolished by fusion with EGFP (40).

Cx40 and Cx45

To examine gating of Cx40/Cx45 junctions, we cocultured HeLa cells expressing Cx40-CFP with those expressing Cx45 and found that JPs readily formed between heterologous cells and that heterologous cell pairs exhibited electrical cell-cell coupling with a mean value for g_j of 4.5 ± 3.1 nS ($n = 28$). The dependence of G_j on V_j was evaluated in response to long V_j ramps as shown in Fig. 3 *A*. Cx40-CFP/Cx45 heterotypic junctions exhibited an asymmetric steady-state G_j-V_j relation similar to that of Cx43-EGFP/Cx45 junctions, i.e., G_j decreased to near zero at relatively negative voltages on the Cx45 side and then increased modestly at larger V_js, exceeding +60 mV (see Fig. 3 *B* and its *inset*). Fig. 3 *C* summarizes data obtained from five cell pairs. Based on the ratio of G_j at $V_j = 0$ mV to that at $V_j = -40$ mV, it would appear that only ~30–40% of the channels are open at $V_j = 0$.

Much like heterotypic Cx43/Cx45 (25) and Cx31/Cx45 (39) junctions, Cx40/Cx45 junctions exhibit signal transfer asymmetry, which can be effectively modulated by the difference in the holding potentials between the cells. In the example shown (Fig. 3 *D*), a Cx45-expressing cell (cell 1) was voltage clamped to −50 mV, and repeated, brief (90 ms) steps ±90 mV in amplitude were applied. The Cx40-expressing cell (cell 2) was maintained in current clamp mode, which permits recording of the coupling potential in cell 2 evoked by voltage steps applied to cell 1. At the start of the recording, depolarizing voltage steps applied to the Cx45 cell were effectively transferred, evident by the voltage responses in cell 2, whereas transfer of hyperpolarizing voltage steps was essentially blocked. Upon progressive depolarization of cell 1, indicated by the vertical arrows, the same repeated steps elicited responses in cell 2 that progressively become more symmetric (compare responses in the period from 0 to 40 s to those from 70 to 80 s). An inset showing recordings in an expanded time scale better illustrates the time course of the changes associated with reversal of the polarity of the voltage steps applied to cell 1. The change in the difference between holding potentials of the two cells, $\Delta V_h = V_1 - V_2$, is plotted in the bottom trace; values were calculated between the repeated pulses. Thus, Cx40/Cx45 like Cx43/Cx45 (25), Cx31/Cx45 (39), or Cx47/Cx45 (Feliksas F. Bukauskas, unpublished) channels demonstrate electrical signal transfer asymmetry, which can be modulated from unidirectional to bidirectional by relatively small changes in ΔV_h.

Cx40 and Cx43

As shown previously in Fig. 1, we examined compatibility between Cx40 and Cx43 using several combinations of cocultured HeLa cells. Examination of 35 cells pairs formed between HeLa cells expressing Cx40 or Cx40-CFP and those expressing Cx43-EGFP showed no cases in which there were well-resolvable JPs, i.e., with sizes exceeding ~1 μm in diameter. Although small fluorescent puncta were observed in regions where heterologous cells were in contact, in no case did these puncta show colocalization of both EGFP and CFP fluorescence (Fig. 1) indicating that they represented

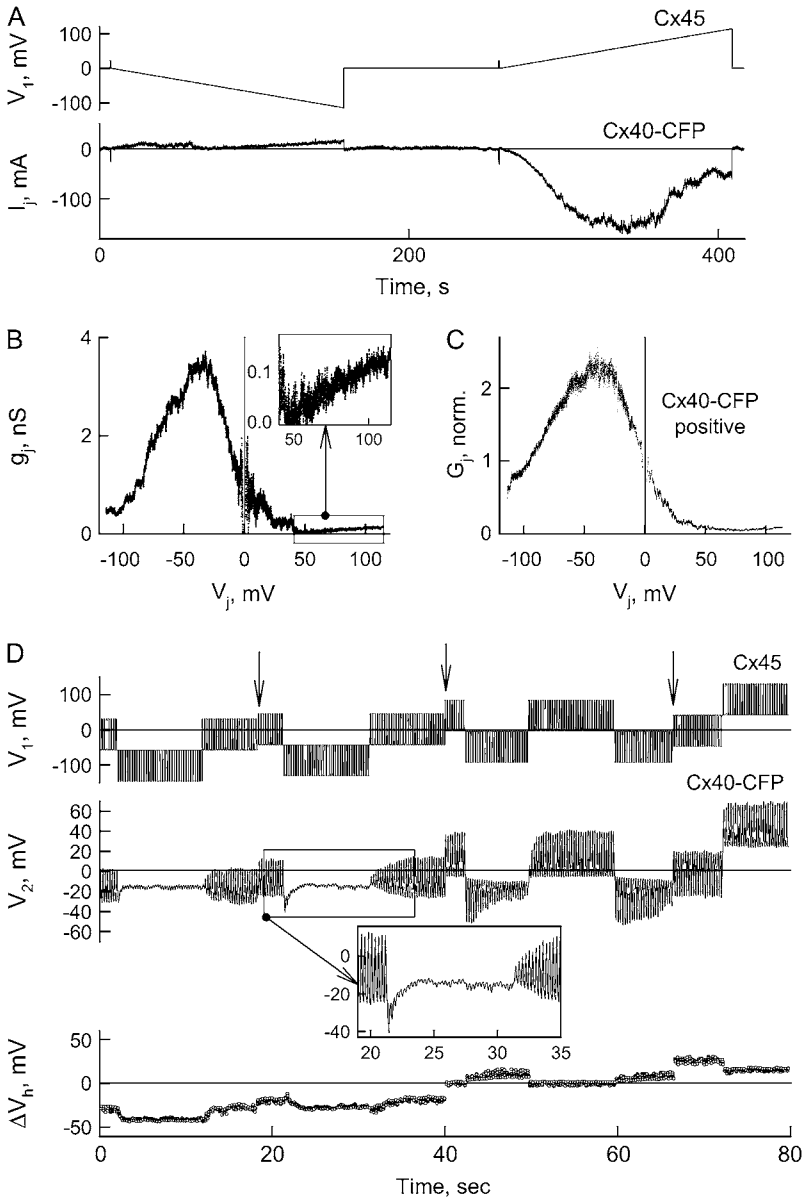

FIGURE 3 Voltage gating and asymmetric signal transfer in heterotypic Cx40/Cx45 junctions. (*A*) Example of an I_j recording in response to long V_j ramps from 0 to −115 mV and from 0 to +115 mV (2.5 min for each ramp) applied to the HeLaCx45 cell of a HeLaCx40-CFP/HelaCx45 cell pair. (*B*) G_j-V_j plot calculated from the record shown in *A* demonstrates gating asymmetry and an increase in g_j (see *inset*) with voltages positive on Cx40-CFP side exceeding ~50 mV. (*C*) Summary of G_j-V_j dependence of Cx40-CFP/Cx45 heterotypic junctions measured in five cell pairs by applying long V_j ramps as shown in *A*. (*D*) Demonstration of signal transfer asymmetry through Cx40-CFP/Cx45 heterotypic junctions. The top trace shows the voltage applied to a HeLa cell expressing Cx45 (cell 1), which was paired with a HeLaCx40-CFP cell; g_j = 1.4 nS. Initially cell 1 was voltage clamped at −50 mV and stepped by ±90 mV for 90 ms with 170 ms between pulses. Cell 2 was in current clamp mode The Cx40-expressing cell (cell 2) was maintained in current clamp mode, which allowed us to record electrotonic potentials evoked by repeated voltage steps applied to cell 1. The initial set of depolarizing and hyperpolarizing voltage pulses (0–18 s) shows substantial asymmetry in the amplitudes of responses in cell-2 depending on the polarity of the pulses. Stepwise depolarization of the holding potential of cell 1 (see *arrows*) leads to a reduction in the degree of signal transfer asymmetry. The bottom trace shows the difference of holding potentials, $\Delta V_h = V_1 - V_2$, during the record.

small heterotypic junctions formed between Cx40-CFP or Cx43-EGFP and an endogenously expressed connexin, presumably Cx45. All cell pairs with small puncta that were examined electrophysiologically demonstrated low levels of coupling. Fig. 4 *A* shows a frequency histogram assembled from Cx40-CFP/Cx43-EGFP heterologous cell pairs. A peak in the Gaussian distribution occurs at $g_j = 1$ nS. All junctions exhibited asymmetry in gating (Fig. 4 *B*) with slightly higher sensitivity when the Cx43-EGFP side was made relatively positive.

In addition, we examined cell-cell coupling between Novikoff cells endogenously expressing Cx43 (41) and HeLaCx40-CFP and neither of 11 randomly selected cell pairs demonstrated functional coupling (data not shown). Our earlier findings demonstrating junction formation and functional coupling between Novikoff and HeLa cells expressing Cx43-EGFP (40), indicate that Novikoff and HeLa cells can form junctions if the Cxs are compatible.

Unitary gating events of heterotypic gap junction channels

Unitary gating events of Cx43/Cx45 channels were described previously (25,42). To characterize gating events associated with Cx40/Cx45 channels, we examined heterologous cell pairs in which one cell expressed Cx40 or Cx40-CFP and the other cell expressed Cx45. Cells expressing wild-type Cx40 or Cx45 were identified by prelabeling with DiI or DAPI. Unitary gating events associated with Cx40(DAPI)/Cx45 heterotypic channels are shown in Fig. 5 *A*. Application of a

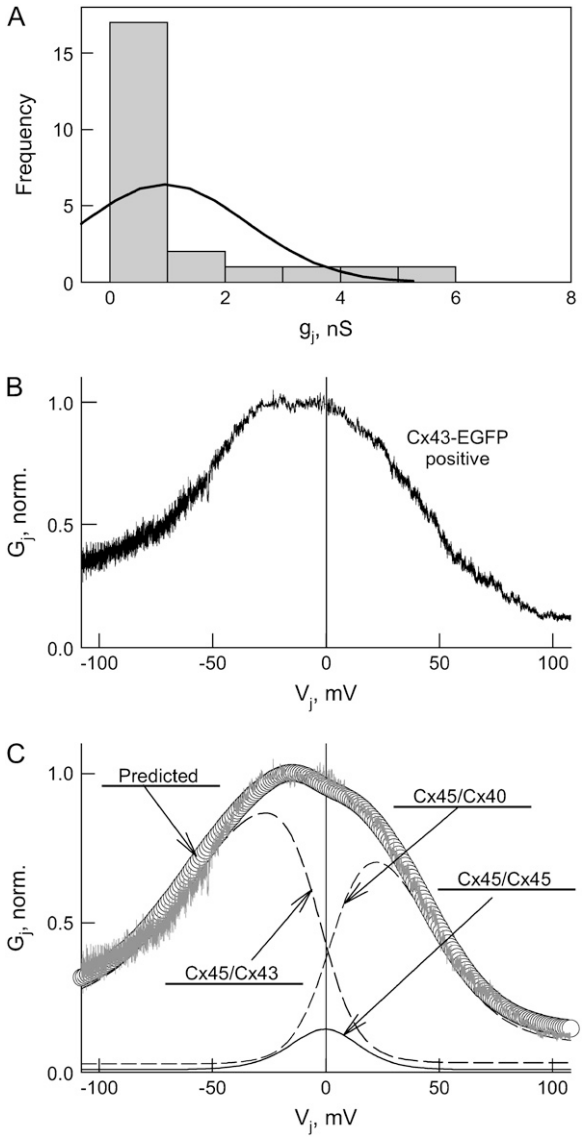

FIGURE 4 Voltage gating in heterologous HeLaCx40-CFP/HelaCx43-EGFP cell pairs. (*A*) Frequency histogram and Gaussian distribution curve of conductances measured in 23 individual cell pairs shows a peak at 1.5 nS. (*B*) G_j-V_j dependence summarized from 5 cell pairs. G_j was measured during long V_j ramps as shown in Fig. 3 *A*. Plot shows higher V_j gating sensitivity with voltages relatively positive on the Cx43-EGFP side. (*C*) Fit of experimental g_j-V_j dependence shown in (*B*) (see *open circles* overlaid over experimental data points) to the sum of two Boltzmann equations describing asymmetric Cx40/Cx45 and Cx43/Cx45 (*dashed lines*) and symmetric Cx45/Cx45 (*solid line*) g_j-V_j dependences.

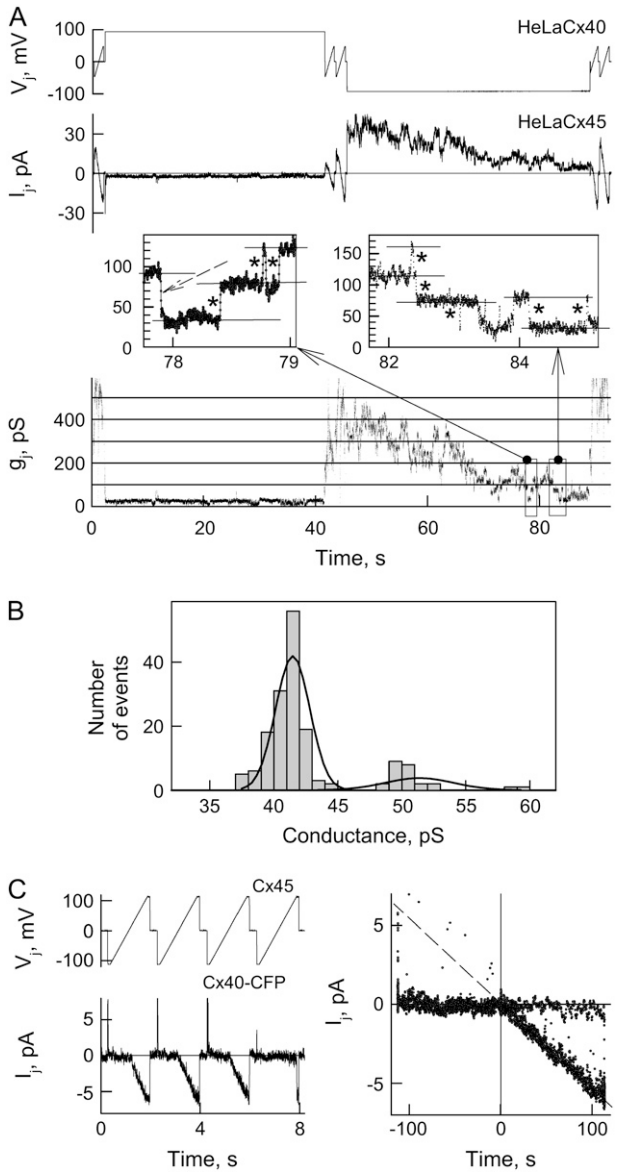

FIGURE 5 Unitary gating events of Cx40/Cx45 heterotypic junctions. (*A*) A representative I_j record from a heterotypic Cx40/Cx45 junction in response to voltage steps and ramps applied to the HeLaCx40 cell; HeLaCx40 cells were prelabeled with DAPI. Two insets show unitary gating events at expanded g_j over time plots. Asterisks show the most frequently observed gating transitions of ~42 pS. A gating event ~53 pS in magnitude is indicated in the left inset by the dashed arrow. (*B*) Data are summarized in a frequency histogram of unitary gating transitions measured in Cx40-CFP or Cx40 (prelabeled with DAPI) and Cx45 heterologous cell pairs. (*C*) An example of V_j and I_j records in a HeLaCx40-CFP/HeLaCx40 cell pair exhibiting single channel activity. The I_j-V_j plot on the right side shows that the channel is mainly closed at V_js relatively negative on Cx45 side and open at opposite polarity. A linear regression line (*dashed line*) fitted to the points corresponding to the open state gives a conductance of ~52 pS.

positive voltage step to the HeLaCx40 cell caused very rapid, full uncoupling, consistent with closure of the highly voltage-sensitive Cx45 hemichannel. Application of a negative voltage step to the same cell produced closure that was less voltage-sensitive. Most of the unitary gating events, shown in two insets, were ~42 pS in magnitude; see gating transitions indicated by asterisks in both insets. Although infrequent, we also observed transitions ~48–58 pS in magnitude (indicated by *dashed arrow* in the *left inset*). Fig. 5 *B* shows a histogram of the amplitudes of unitary gating transitions, which were calculated from three Cx40/Cx45 and five Cx40-CFP/Cx45 cell pairs. A fit of the frequency

histogram to Gaussian functions (*solid lines*) resulted in two peaks at ~42 and 52 pS. Each event was defined as a transition between different conductance states, where the residence time in each state was at least 20 ms. Fig. 5 *C* show V_j and I_j records from a Cx40-CFP/Cx45 cell pair when a V_j ramp (from −112 to 112 mV) was applied to the Cx45 cell and only one channel was operational during recovery from CO_2 application. The I_j trace shows fast channel closure when the Cx45 side is relatively negative and reopening upon reversing the polarity of V_j. The I/V plot from this record is shown on the right. The steepness of the linear regression line derived from the points that correspond to the open state (see *dashed line*) indicated a conductance of 53 pS. This conductance is close to that predicted by the series arrangement of Cx45 and Cx40 hemichannels assuming that their conductances are twice that of the corresponding cell-cell channels, i.e., 64 and 300 pS ($64 \times 300/(64 + 300) =$ 52.7 pS) (25,43). Thus, we attribute the ~52 pS peak in the histogram to gating events between the fully open (main) state and the closed state and the ~42 pS peak to gating events between the main open state and substate(s); the latter transitions dominate at the V_j that was applied. It has been suggested that the unitary conductance of Cx40/Cx45 channels is ~40 pS (44), which likely corresponds to the transitions between the main open state and substate(s). Both macroscopic (see Fig. 3 *C*) and single channel records (see Fig. 5 *A*) support the view that Cx40 gates at negativity on its cytoplasmic side. Most of the gating transitions were between the open state and substate(s) suggesting that macroscopic V_j gating of Cx40 hemichannels largely reflects the fast V_j gating mechanism. Gating between fully open and closed states is present, but is substantially less (~10-fold) frequent. Therefore, we conclude that both gates of Cx40 exhibit negative gating polarity, but the slow gating mechanism is substantially less sensitive to V_j than the fast one.

Since pairing HeLa cells expressing Cx40 with those expressing Cx43 exhibit low levels of coupling, but no evidence that Cx40 and Cx43 form JPs, we examined the unitary gating events at the single channel level to determine whether the channel properties are consistent with Cx43/Cx45, Cx40/Cx45 and/or Cx45/Cx45 channels, as well as perhaps heteromeric forms of these Cxs. Fig. 6 *A* shows a typical example of an I_j record in response to voltage steps and ramps (V_j trace) applied to the Cx40-CFP-expressing cell of a Cx40-CFP/Cx43-EGFP cell pair. Unitary gating events from several channels were resolvable without pharmacological intervention. V_j steps of both polarities (±100 mV) tended to ultimately cause full uncoupling, but with higher apparent V_j sensitivity with steps relatively positive on Cx43-EGFP side, consistent with the G_j-V_j dependence observed macroscopically (see Fig. 4 *A*). A simple series arrangement of Cx43 and Cx40 hemichannels would predict a unitary conductance for a Cx43/Cx40 heterotypic channel of ~130 pS. However, we, as well as others (21) who also used HeLa transfectants, did not observe a unitary conductance in this

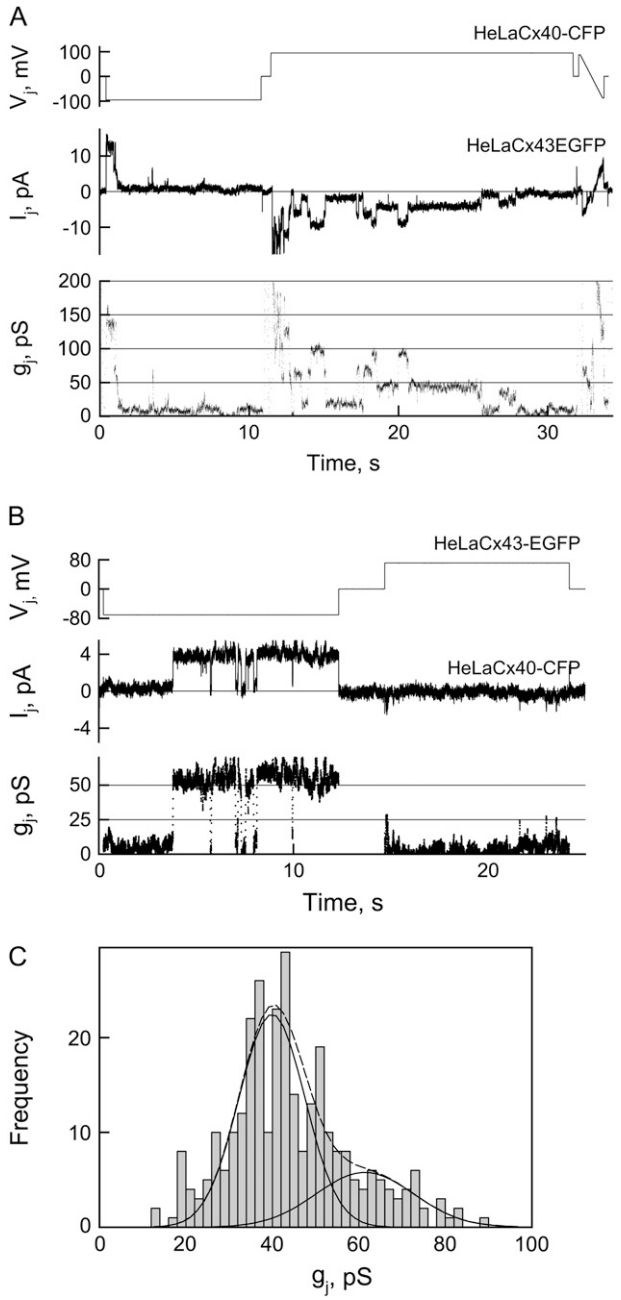

FIGURE 6 Unitary gating events in Cx40/Cx43 heterologous cell pairs. (*A*) Unitary gating events recorded in a HeLaCx43-EGFP/HeLaCx40-CFP cell pair during voltage steps and ramps applied to the HeLaCx40-CFP cell. (*B*) An example of a single channel record in a HeLaCx43-EGFP/HeLaCx40-CFP cell pair. (*C*) Data are summarized in a frequency histogram of unitary gating transitions measured in Cx40-CFP and Cx43-EGFP heterologous cell pairs.

range. Fig. 6 *B* shows an example of a recording from a Cx43-EGFP/Cx40-CFP heterologous cell pair in which only one channel was active. During a negative voltage step applied to the HeLaCx43-EGFP cell, the channel gates between fully open and closed states with a conductance size of ~54 pS. A voltage step of opposite polarity caused very

rapid full uncoupling. The conductance and gating characteristics of this channel bear close resemblance to those we reported for Cx43-EGFP/Cx45 channels (25) or for Cx40/Cx45 channels reported here (Fig. 5).

Fig. 6 *C* summarizes data of unitary gating events obtained from 18 Cx40-CFP/Cx43-EGFP cell pairs. A frequency histogram shows that the amplitudes of the unitary gating events were spread out from ~20 pS to ~90 pS, with a majority of the transition sizes falling between 30 pS and 60 pS. A fit of the frequency histogram to multiple Gaussian functions suggest two plausible peaks at ~40 pS and ~62 pS (*solid lines*); the dashed line is a composite of the two Gaussian functions. Possible channels within this conductance range are Cx45 homotypic channels as well as Cx40/Cx45 and Cx43/Cx45 heterotypic channels. The conductances in the range of ~60–90 pS probably represent a heteromeric channels composed of Cx45 and Cx43 or Cx40. Each of these channels can also show substate gating, with subconductance transitions ~75% that of the open state. The presence of substates, as well as the possibility that heteromeric channels form, would lead to smearing of the histogram and poor distinction of peaks associated with each channel type. Heteromeric channels have been shown to form between Cx45 and Cx43 (45). Reported data regarding function of heteromeric channels formed of Cx40 and Cx43 are not in agreement (46,47).

DISCUSSION

Expression patterns of connexins in different tissues suggest that heterotypic and heteromeric channels likely form and contribute to electrical and metabolic communication between cells. We focused our studies on Cx40, Cx43, and Cx45, which are principal cardiac Cxs forming GJs between cardiomyocytes of the conduction system and working myocardium of atria and ventricles. Cx45, along with the recently identified mCx30.2 GJ protein, is most abundantly expressed in the sinoatrial and atrioventricular nodes (5). Cx40 is expressed in the atria and the conduction system of ventricles, whereas Cx43 is a major Cx forming GJs between working cardiomyocytes (48). These distinct expression patterns are important for synchronous excitation of cells inside atria and ventricles and for imparting a substantial AV delay that is vital for efficient mechanical function of the heart (9).

It is not well established whether the incompatibility of particular Cx isoforms to form heterotypic junctions resulted from evolutionary directed necessity to perform a specific function. We speculate that this property could affect not only electrical and metabolic communication in the adult tissue but also cell differentiation during development. Typically, most embryonic cells express one or several Cx isoforms, and strong connexin-mediated cell-cell coupling tends to eliminate intercellular gradients of diffusible substances, which include ions, metabolites, small peptides, oligonucleotides and small interfering RNA (siRNA) (2,49,50). Thus, in order for neighboring cell populations to develop independently it may be important to express connexin isoforms that cannot form heterotypic junctions, thereby impairing electrical synchronization, transfer of signaling molecules or metabolic communication between different cell populations while maintaining communication within the same cell types. It is possible that expression of Cx40 by cells forming the His bundle, its branches and terminal network of Purkinje fibers at early stages of development facilitates their differentiation into the conductive system independent from working cardiomyocytes of ventricles expressing mainly Cx43. This functional separation may ultimately lead to anatomical separation, e.g., by a layer of connective tissue in between them. Ultimately, excitation must be transferred from the conduction system to the working myocardium and the appearance of Cx43 expression in parallel to Cx40 in the distal segment of the bundle branches (6) could serve this function at the transitions formed at Purkinje-muscle (P-M) connections (51) discretely distributed on the endocardium surface with ~1.5 mm distance between them (52). Presumably Cx43 homotypic GJs are responsible for signal transfer in P-M connections. Thus, expression of incompatible connexins can assist in cell differentiation and also limit interaction between functionally different systems if they are not yet anatomically separated. A similar mechanism may explain development of endothelium, which mainly expresses Cx40, and smooth muscle cell layers, which mainly express Cx43, in the blood vessels.

Heterotypic compatibility among Cx40, Cx43, and Cx45

Originally, electrophysiological studies in *Xenopus* oocytes (10) reported that Cx40 and Cx43 do not form functional heterotypic channels. This conclusion is supported by Gu et al. (27). A similar conclusion was reached using HeLa transfectants in studies that showed a lack of dye transfer (53) and a lack of electrical cell-cell coupling (26); in the latter study, there was also no evidence that Cx40/Cx43 JPs formed when stained with Cx-specific antibodies suggesting that Cx40 and Cx43 hemichannels do not dock or cluster into JPs. However, subsequent studies, performed in HeLa and RIN cell transfectants reported low levels of functional coupling attributed to Cx40/Cx43 heterotypic channels (21,22). Both studies concluded that Cx40/Cx43 channels are functional despite reporting differences in properties such as V_j gating, single channel conductance and open channel current rectification. Cotrell and Burt (22) commented that the differences regarding voltage gating properties could be due to the short duration (~0.5 s) of the voltage pulses used in (21) to characterize steady-state g_j-V_j dependence and stated that by using this protocol they may have characterized ''fast inactivation while changes in slow inactivation were not assessed''. It may be that the differences in these studies arise from expression of different intrinsic Cxs in HeLa and

RIN cells. Given the potential importance of Cx40 and Cx43 compatibility in the cardiovascular system, the CNS, and other organs, we reexamined this issue, taking advantage of GFP-tagged connexins that allowed us to visualize JP formation and record electrophysiologically from the same cell pairs. The pattern of compatibility using Cxs tagged with color variants of GFP is the same as that reported by Haubrich et al. (26) using wild-type Cxs. In addition, studies performed in *Xenopus* oocytes demonstrated lack of coupling between oocytes expressing untagged forms of Cx40 and Cx43 (10,27). Thus, GFP tags should not affect the property of hemichannels to dock and form functional GJ channel.

We conclude that Cx40 and Cx43 are incompatible and that the failure to observe functional Cx40/Cx43 heterotypic channels results from an inability of the component hemichannels to dock and/or to cluster into JPs. This conclusion is supported by several observations. In cocultures of HeLa cells expressing Cx40-CFP and Cx43-EGFP we never observed colocalization of CFP and EGFP at identifiable JPs or at any fluorescent puncta in the junctional membrane. What we did observe often were small (<1 μm) fluorescent puncta in the junctional membrane that were always of one color indicating that they were not formed by the pairing of Cx40 with Cx43 (see Fig. 1, *D* and *E*). Also, the presence of these puncta was accompanied by low levels of coupling comparable in magnitude with g_j measured between HeLa cells expressing Cx40 or Cx43 and HeLa parental cells and by asymmetric V_j gating. In addition, the unitary conductances are significantly below to those predicted ($\sim$130 pS) for a heterotypic Cx40/Cx43 GJ channel.

Electrophysiological examination of heterologous Cx40-CFP/Cx43-EGFP and Cx40/Cx43-EGFP cell pairs containing small fluorescent puncta revealed a mean g_j of $\sim$1 nS and asymmetric V_j gating. Given that we propose that this coupling is mediated by interactions with Cx45, the low values of g_j are explainable by the low levels of available endogenous Cx45. The asymmetry in voltage dependence is also explainable through combinations of Cx43-EGFP/Cx45 and Cx40-CFP/Cx45 heterotypic channels mixed in with homotypic Cx45 channels. To assess whether the presence of intrinsically expressed Cx45 can account for the experimentally observed data, we fitted the experimentally obtained g_j-V_j dependence shown in Fig. 4 *B* to the sum of Boltzmann equations describing g_j-V_j dependencies of Cx40/Cx45, Cx43/Cx45, and Cx45/Cx45 junctions (see Fig. 4 *C*). For simplicity, we described g_j-V_j dependence of any given junction by multiplying two Boltzmann equations, each describing gating of one of the hemichannels, e.g., $G_j = \{g_{min,1} + (1 - g_{min,1})/(1 + \exp(A_1 \times (V_j - V_{o,1})))\} \times \{g_{min,2} + (1 - g_{min,2})/(1 + \exp(A_2 \times (-V_j - V_{o,2})))\}$, where g_{min}, A, and V_o are Boltzmann constants, and subscripts 1 and 2 correspond to each of two hemichannels. For Cx45 homotypic junctions, $g_{min,1} = g_{min,2}$, $A_1 = A_2$, and $V_{o,1} = V_{o,2}$. The two dashed lines represent the asymmetric G_j-V_j relations of Cx45/Cx43 and Cx45/Cx40 heterotypic junctions derived from the fitting. These two junctions would be situated in opposite orientations. We acknowledge that description of heterotypic junctions by multiplying two Boltzmann equations is approximate even though they closely describe the G_j-V_j relationships shown in Figs. 2 *A* and 3 *C*. The solid line represents Cx45 homotypic junctions. Thus, Fig. 4 *C* illustrates that HeLaCx40/HeLaCx43 cell pairs can exhibit g_j-V_j gating with moderate V_j gating sensitivity and asymmetry even when composed of Cx40/Cx45 and Cx43/Cx45 heterotypic junctions, each exhibiting strong V_j gating asymmetry.

Examination of unitary events in Cx43-EGFP/Cx40-CFP cells pairs revealed a relatively broad distribution of conductance transitions ranging from 20 pS to 90 pS. This distribution is plausible given the number of potential channel types that can form, such as Cx45 homotypic junctions, Cx40/Cx45 and Cx43/Cx45 heterotypic junctions, and a number of heteromeric forms assembled from Cx43 and Cx45 (45). A simple series arrangement of Cx43 and Cx40 hemichannels would predict a unitary conductance of $\sim$130–140 pS. The lack of gating transitions exceeding 90 pS supports our assertion that Cx40/Cx43 heterotypic channels do not form.

Voltage gating and cell-to-cell signaling asymmetry of heterotypic junctions

A property common to GJ channels formed of all Cxs is sensitivity of g_j to V_j (54–56). A common feature reported for V_j gating is that steady-state g_j does not decline to zero with increasing V_j, but reaches a plateau or residual conductance that varies from $\sim$5% to 30% of the maximum g_j depending on the Cx isoform. Single channel studies showed that the residual g_j is due to incomplete closure of the GJ channels by V_j (57,58). Gating to different levels via distinct fast and slow gating transitions led to the finding that there are two different types of V_j sensitive gates (see Fig. 7 *A*). One, termed the fast V_j gate, is characterized by transitions between open and residual conductance states, and the other, termed the slow V_j or ''loop'' gate, is characterized by transitions between open and fully-closed states (reviewed in Verselis et al. (56)). Mutational studies demonstrated that the gating polarity of the fast gating mechanism is governed by charged residues in the N-terminal domain (59,60). Modifications of Cx43, including deletion of the CT domain (24) or attachment of aequorin or EGFP to CT, selectively abolishes fast gating to the residual state (61,62). Taken together, these data demonstrate that there are two molecularly distinct gating mechanisms in each hemichannel.

Gating in heterotypic junctions is typically asymmetric with respect to $V_j = 0$ and the degree of asymmetry depends on the intrinsic gating properties of the component hemichannels. Cx45 homotypic junctions exhibit the highest V_j gating sensitivity among all members of the connexin family and this property contributes to the high degree of V_j gating

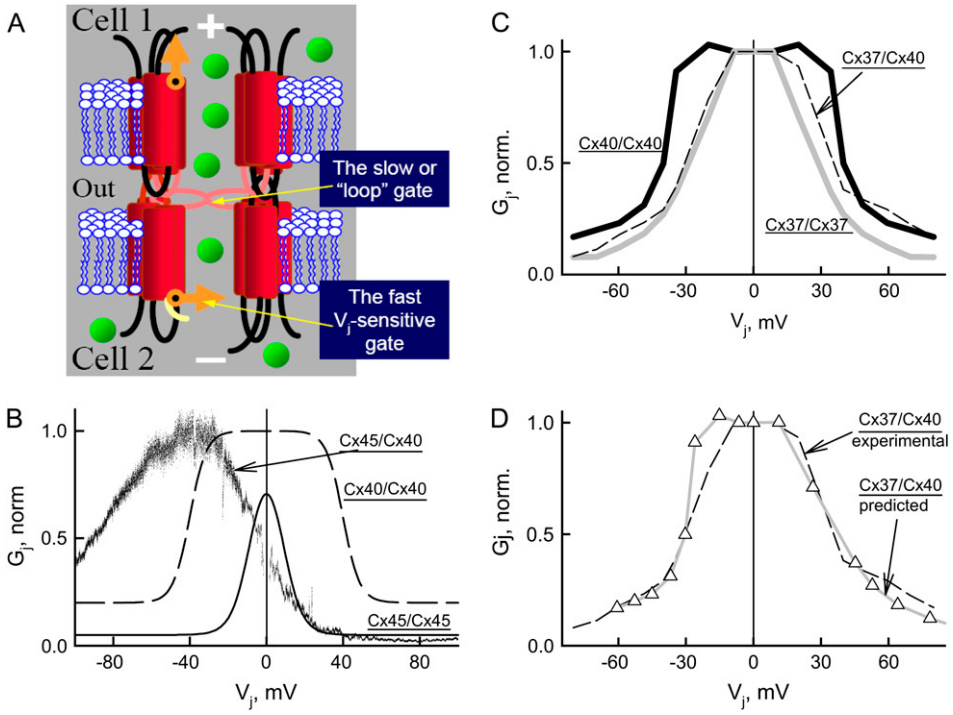

FIGURE 7 Cx40 hemichannels close upon relative negativity on their cytoplasmic side. (*A*) Schematic illustration of a gap junction channel embedded in two lipid bilayers. The putative fast and slow gates are depicted to be in closed states in the hemichannel at the bottom. (*B*) Superposition of a G_j-V_j plot of a Cx40/Cx45 heterotypic junction (from Fig. 3 *C*) with G_j-V_j plots of Cx40 (*dashed line*) and Cx45 (*solid line*) homotypic GJs. (*C*) Solid lines show G_j-V_j dependences of Cx40 (*black*) and Cx37 (*gray*) homotypic junctions, whereas dashed line shows G_j-V_j dependence of Cx37/Cx40 heterotypic junction (adopted from Bruzzone et al. (10)). (*D*) Superposition of the experimental G_j-V_j plot of the Cx37/Cx40 heterotypic junction (*dashed line*; the same as shown in *C*) and a theoretical G_j-V_j plot (*solid line* with *triangles*) predicted from G_j-V_j plots of homotypic Cx37 and Cx40 junctions (shown in *C*) by assuming that the voltage drop across the Cx40 hemichannel is twice that across the Cx37 hemichannel and that both Cxs close at negativity on their cytoplasmic side.

asymmetry in all heterotypic junctions containing Cx45 on one side, such as mCx30.2/Cx45 (5), Cx31/Cx45 (39), Cx43/Cx45 (25), and Cx40/Cx45 (see Fig. 3 *C*). In all cases, there is higher V_j gating sensitivity when the Cx45 side is made relatively negative, which has been shown to result predominantly from closure of the slow gate of the Cx45 hemichannel (25). The fast gate of Cx45 also closes for this polarity, but its voltage sensitivity is shifted to higher V_js. The fast and slow V_j-sensitive gates of Cx43 GJs also close on relative negativity. Previously, we reported that differences in the unitary conductances of the component hemichannels resulted in a higher V_j gating asymmetry in Cx43/Cx45 junctions than that predicted by the simple docking of two hemichannels exhibiting equal unitary conductances. Most of the V_j applied across a Cx43/Cx45 channel falls across the Cx45 hemichannel, which has ~3.5-fold smaller conductance than the Cx43 hemichannel, resulting in increased and decreased V_j gating sensitivities of Cx45 and Cx43 hemichannels, respectively (25).

Fig. 7 *B* shows the G_j-V_j dependence of Cx40/Cx45 heterotypic junction (from Fig. 3 *C*; G_j normalized to 1) superposed onto G_j-V_j plots of Cx40 and Cx45 homotypic GJs; Boltzmann parameters for these two plots were derived from earlier reports (43,63). Given that the gating polarity of the Cx45 hemichannel is negative, we attribute G_j decay at negative V_js (negativity on Cx40 side) to closure of the Cx40 hemichannel and G_j decay in V_j range from ~−20 to +100 mV to the closure of the Cx45 hemichannel. Thus, the G_j-V_j dependence of Cx45/Cx40 heterotypic junctions allows us to conclude that the gating polarity of the Cx40 hemichannel is negative. In addition, it follows from Fig. 7 *B* that V_j sensitivity of the Cx40 hemichannel is reduced, whereas V_j sensitivity of the Cx45 hemichannel is enhanced that is in agreement with the view that the difference in the unitary conductances of the component hemichannels influences the G_j-V_j relation.

In earlier studies, based on V_j gating asymmetry in pairs of *Xenopus* oocytes forming Cx37/Cx40 heterotypic junctions, the gating polarity of Cx40 was predicted to be positive (10,64). In Fig. 7 *C*, gray and black solid lines show g_j-V_j dependences of Cx37 and Cx40 homotypic junctions, respectively, obtained from (10). Based on the correspondence of G_j-V_j dependence of Cx37/Cx40 heterotypic junctions (*dashed line* in Fig. 7 *C*) at negative V_js with that of Cx37, and g_j decay for both polarities of V_j, it was concluded that both Cx37 and Cx40 hemichannels close on positivity on their cytoplasmic sides. At that time, the single channel conductances of Cx37 and Cx40 were not known. It turns out that the single channel conductance of Cx37 is very large, ~300 pS or more (65), which is ~2-fold higher than that of Cx40 (43). Thus, a higher fraction of V_j would drop across the higher-resistance Cx40 hemichannel, resulting in higher and lower apparent sensitivities to V_j for Cx40 and Cx37 hemichannels, respectively. Fig. 7 *D* shows superposition of the experimental g_j-V_j plot of a Cx37/Cx40 heterotypic junction (*dashed line*; from Bruzzone et al. (10)) and theoretical g_j-V_j plot (see *solid line* with *triangles*) predicted with data obtained from homotypic Cx40 and Cx37 junctions assuming that voltage drop across the Cx40 hemichannel is twice of that across the Cx37 hemichannel and that the Cxs

close at negativity on their cytoplasmic sides. To evaluate correspondence between experimental and theoretical data, we calculated the sum of squared deviations, $\Sigma(\Delta G_j^2)$, between two sets of data at all measured V_js and found that $\Sigma(\Delta G_j^2) = 0.19 \pm 0.18$. We also calculated a g_j-V_j plot (not shown) assuming that both Cxs close on positivity and found that $\Sigma(\Delta G_j^2) = 0.33 \pm 0.11$. Thus, the assumption that Cx40 and Cx37 possess negative gating polarities provides a 1.7-fold better fit to experimental data. Even though our analysis suggests that gating polarity of Cx37 should be negative, we cannot exclude the possibility that the fast or the slow gate of Cx37 possesses positive gating polarity. Based on the absence of V_j gating in Cx40/Cx43 and Cx40/Cx45 cell pairs at relative negativity on Cx40 side, it was reported that Cx40 gates at positivity on its cytoplasmic side (21); bipolar V_j steps of 0.5 s in duration were used for V_j gating studies. These data do not contradict ours because as follows from Figs. 2 *A* and 3 *C*, a substantial fraction of channels are closed at $V_j = 0$ mV and application of V_j steps positive on Cx45 side should result in an initial increase in g_j, and would only show a decay with longer V_j steps. To examine the g_j-V_j relation of Cx40/Cx45 GJs, we used voltage steps ~30 s in duration and voltage ramps ~150 s in duration. We observed substantial reductions in g_j at V_js negative on Cx40 side both at macroscopic (see Fig. 3 *C*) and single channel levels (see Fig. 5 *A*). Similarly, it was shown that V_j gating occurs at negativity on the Cx40 side in Cx40/Cx43 cell pairs when V_j steps of 30 s in duration were used (22). Thus, we conclude that Cx40 has a negative gating polarity, like Cx45 and Cx43 hemichannels. Furthermore, our experimental data at the single channel level (Fig. 5) demonstrate gating transitions of ~52 pS that we attribute to gating between open and closed states and those of ~42 pS that we attribute to gating between open and residual states. Therefore, gating polarities of both slow and fast V_j gating mechanisms of Cx40 are negative.

Thus far, all heterotypic junctions that contain a Cx45 hemichannel on one side (Cx40/Cx45, Fig. 3 *B*; Cx43/Cx45, Fig. 2 *A*; Cx31/Cx45, Fig. 3 *B* in Abrams et al. (39)) show a strong decrease in g_j when V_j is stepped from 0 to ~40 mV relatively negative on the Cx45 side. A subsequent increase in g_j occurs with V_js exceeding 40 mV. Two mechanisms can contribute to this increase in conductance: 1), interactions between the two series gates in the Cx45 hemichannel (66); and 2), the rectification of the residual state of the Cx45 hemichannel demonstrated in the Fig. 2 *C*. Rectification of the residual state is a property that has been described in other connexins, such as Cx32 and Cx43, and has been proposed to result from introduction of charge asymmetry in the pore as a result of conformational changes associated with one hemichannel gating (37,38).

Earlier we reported that the strong g_j-V_j gating asymmetry of Cx43/Cx45 (25) and Cx31/Cx45 (39) heterotypic junctions produces signal transfer asymmetry that can be increased or decreased by making the cell expressing Cx45 relatively more negative or positive, respectively. In Fig. 3 *D*, we show that a similar phenomenon occurs in Cx40/Cx45 junctions. Variations of ΔV_h of around zero very effectively modulate the degree of asymmetry, and at ΔV_h ~20 mV positive on the Cx40-EGFP side, electrical coupling is almost unidirectional for signals comparable in amplitude to action potentials. Thus, a synapse with Cx45 on the presynaptic side and Cx40 on the postsynaptic side could be highly rectifying. Transmission at synapses using this mechanism would differ from known electrical synapses that are involved in escape systems, where the rectification is very rapid (τ = ~1 ms (67–69)), and presumably is caused by single channel rectification or very fast gating. It is interesting that in all described rectifying synapses the presynaptic neuron is at more negative resting potential ((70) and reviewed in (71)) resulting in ΔV_h of ~15 mV. Therefore, cell-to-cell signaling asymmetry seems to be a common feature of heterotypic junctions containing a Cx45 hemichannel on one side. Such signaling asymmetry may be functionally relevant in the CNS where signal propagation in one direction is preferred; Cx45 expression has been reported in neurons of the olivocerebellar system, in spinal motor neurons and in the ganglion cell and inner nuclear layers of mouse retina (12,72,73). For example, if orthodromic propagation is from the cell expressing Cx45 (presynaptic, if considering an electrical synapse) to the cell expressing Cx40 or Cx43, one would expect antidromic propagation to be drastically reduced (see Fig. 3 *D*) due to the slow gate of the Cx45 hemichannel, which closes the channels fully. In addition, it may explain, at least in part, differences in the velocity of the spread of excitation in antero- and retrograde directions in sinoatrial (7,8) and AV-nodal regions of the heart.

SUPPLEMENTARY MATERIAL

An online supplement to this article can be found by visiting BJ Online at http://www.biophysj.org.

We thank Dr. Angele Bukauskiene for excellent technical assistance.

This work was supported by grants from the National Institutes of Health and the German Research Association, RO1 NS036706 to F.F.B., MH66199 to V.K.V. and Wi 270/25-1,2 to K.W.

REFERENCES

1. Paul, D. L. 1986. Molecular cloning of cDNA for rat liver gap junction protein. *J. Cell Biol.* 103:123–134.
2. Harris, A. L. 2001. Emerging issues of connexin channels: biophysics fills the gap. *Q. Rev. Biophys.* 34:325–472.
3. Sohl, G., and K. Willecke. 2004. Gap junctions and the connexin protein family. *Cardiovasc. Res.* 62:228–232.
4. Severs, N. J., E. Dupont, S. R. Coppen, D. Halliday, E. Inett, D. Baylis, and S. Rothery. 2004. Remodelling of gap junctions and connexin expression in heart disease. *Biochim. Biophys. Acta.* 1662: 138–148.

5. Kreuzberg, M. M., G. Sohl, J. Kim, V. K. Verselis, K. Willecke, and F. F. Bukauskas. 2005. Functional properties of mouse connexin 30.2 expressed in the conduction system of the heart. *Circ. Res.* 96:1169–1177.
6. Gros, D. B., and H. J. Jongsma. 1996. Connexins in mammalian heart function. *Bioessays.* 18:719–730.
7. Coppen, S. R., E. Dupont, S. Rothery, and N. J. Severs. 1998. Connexin45 expression is preferentially associated with the ventricular conduction system in mouse and rat heart. *Circ. Res.* 82:232–243.
8. Verheijck, E. E., M. J. van Kempen, M. Veereschild, J. Lurvink, H. J. Jongsma, and L. N. Bouman. 2001. Electrophysiological features of the mouse sinoatrial node in relation to connexin distribution. *Cardiovasc. Res.* 52:40–50.
9. Kreuzberg, M. M., K. Willecke, and F. Bukauskas. 2006. Connexin-mediated cardiac impulse propagation: connexin 30.2 slows atrioventricular conduction in mouse heart. *Trends Cardiovasc. Med.* 16:266–272.
10. Bruzzone, R., J. A. Haefliger, R. L. Gimlich, and D. L. Paul. 1993. Connexin40, a component of gap junctions in vascular endothelium, is restricted in its ability to interact with other connexins. *Mol. Biol. Cell.* 4:7–20.
11. Nagasawa, K., H. Chiba, H. Fujita, T. Kojima, T. Saito, T. Endo, and N. Sawada. 2006. Possible involvement of gap junctions in the barrier function of tight junctions of brain and lung endothelial cells. *J. Cell. Physiol.* 208:123–132.
12. Van Der Giessen, R. S., S. Maxeiner, P. J. French, K. Willecke, and C. I. De Zeeuw. 2006. Spatiotemporal distribution of Connexin45 in the olivocerebellar system. *J. Comp. Neurol.* 495:173–184.
13. Kirchhoff, S., J. S. Kim, A. Hagendorff, E. Thonnissen, O. Kruger, W. H. Lamers, and K. Willecke. 2000. Abnormal cardiac conduction and morphogenesis in connexin40 and connexin43 double-deficient mice. *Circ. Res.* 87:399–405.
14. Verheule, S., C. A. van Batenburg, F. E. Coenjaerts, S. Kirchhoff, K. Willecke, and H. J. Jongsma. 1999. Cardiac conduction abnormalities in mice lacking the gap junction protein connexin40. *J. Cardiovasc. Electrophysiol.* 10:1380–1389.
15. Kruger, O., A. Plum, J. S. Kim, E. Winterhager, S. Maxeiner, G. Hallas, S. Kirchhoff, O. Traub, W. H. Lamers, and K. Willecke. 2000. Defective vascular development in connexin 45-deficient mice. *Development.* 127:4179–4193.
16. Liao, Y., K. H. Day, D. N. Damon, and B. R. Duling. 2001. Endothelial cell-specific knockout of connexin 43 causes hypotension and bradycardia in mice. *Proc. Natl. Acad. Sci. USA.* 98:9989–9994.
17. Kirchhoff, S., E. Nelles, A. Hagendorff, O. Kruger, O. Traub, and K. Willecke. 1998. Reduced cardiac conduction velocity and predisposition to arrhythmias in connexin40-deficient mice. *Curr. Biol.* 8: 299–302.
18. van Rijen, H. V., T. A. van Veen, M. J. van Kempen, F. J. Wilms-Schopman, M. Potse, O. Krueger, K. Willecke, T. Opthof, H. J. Jongsma, and J. M. de Bakker. 2001. Impaired conduction in the bundle branches of mouse hearts lacking the gap junction protein connexin40. *Circulation.* 103:1591–1598.
19. Bagwe, S., O. Berenfeld, D. Vaidya, G. E. Morley, and J. Jalife. 2005. Altered right atrial excitation and propagation in connexin40 knockout mice. *Circulation.* 112:2245–2253.
20. de Wit, C., S. E. Wolfle, and B. Hopfl. 2006. Connexin-dependent communication within the vascular wall: contribution to the control of arteriolar diameter. *Adv. Cardiol.* 42:268–283.
21. Valiunas, V., R. Weingart, and P. R. Brink. 2000. Formation of heterotypic gap junction channels by connexins 40 and 43. *Circ. Res.* 86: E42–E49.
22. Cottrell, G. T., and J. M. Burt. 2001. Heterotypic gap junction channel formation between heteromeric and homomeric Cx40 and Cx43 connexons. *Am. J. Physiol. Cell Physiol.* 281:C1559–C1567.
23. Valiunas, V., E. C. Beyer, and P. R. Brink. 2002. Cardiac gap junction channels show quantitative differences in selectivity. *Circ. Res.* 91: 104–111.
24. Elenes, S., A. D. Martinez, M. Delmar, E. C. Beyer, and A. P. Moreno. 2001. Heterotypic docking of Cx43 and Cx45 connexons blocks fast voltage gating of Cx43. *Biophys. J.* 81:1406–1418.
25. Bukauskas, F. F., A. Bukauskiene, V. K. Verselis, and M. V. L. Bennett. 2002. Coupling asymmetry of heterotypic connexin 45/connexin 43-EGFP gap junctions: properties of fast and slow gating mechanisms. *Proc. Natl. Acad. Sci. USA.* 99:7113–7118.
26. Haubrich, S., H. J. Schwarz, F. Bukauskas, H. Lichtenberg-Frate, O. Traub, R. Weingart, and K. Willecke. 1996. Incompatibility of connexin 40 and 43 Hemichannels in gap junctions between mammalian cells is determined by intracellular domains. *Mol. Biol. Cell.* 7:1995–2006.
27. Gu, H., J. F. Ek-Vitorin, S. M. Taffet, and M. Delmar. 2000. Coexpression of connexins 40 and 43 enhances the pH sensitivityof gap junctions: a model for synergistic interactions among connexins. *Circ. Res.* 86:E98–E103.
28. Moreno, A. P. 2004. Biophysical properties of homomeric and heteromultimeric channels formed by cardiac connexins. *Cardiovasc. Res.* 62:276–286.
29. Thomas, N., E. Dupont, D. Halliday, C. Fry, and N. J. Severs. 2005. Compatibility, Ratio of Co-Expression and Functional Analysis of Connexins Expressed in the Heart using a New Inducible Cell Model. Whistler, British Columbia, Canada. 59.
30. Jordan, K., J. L. Solan, M. Dominguez, M. Sia, A. Hand, P. D. Lampe, and D. W. Laird. 1999. Trafficking, assembly, and function of a connexin43-green fluorescent protein chimera in live mammalian cells. *Mol. Biol. Cell.* 10:2033–2050.
31. Bukauskas, F. F. 2001. Inducing de novo formation of gap junction channels. *Methods Mol. Biol.* 154:379–393.
32. Neyton, J., and A. Trautmann. 1985. Single-channel currents of an intercellular junction. *Nature.* 317:331–335.
33. White R. L., D. C. Spray, C. A. C. Campos de, B. A. Wittenberg, and M. V. Bennett. 1985. Some electrical and pharmacological properties of gap junctions between adult ventricular myocytes. *Am. J. Physiol.* 249:C447–C455.
34. Butterweck, A., U. Gergs, C. Elfgang, K. Willecke, and O. Traub. 1994. Immunochemical characterization of the gap junction protein connexin45 in mouse kidney and transfected human HeLa cells. *J. Membr. Biol.* 141:247–256.
35. Hulser, D. F., B. Rehkopf, and O. Traub. 1997. Dispersed and aggregated gap junction channels identified by immunogold labeling of freeze-fractured membranes. *Exp. Cell Res.* 233:240–251.
36. Harris, A. L., D. C. Spray, and M. V. Bennett. 1981. Kinetic properties of a voltage-dependent junctional conductance. *J. Gen. Physiol.* 77:95–117.
37. Oh, S., J. B. Rubin, M. V. Bennett, V. K. Verselis, and T. A. Bargiello. 1999. Molecular determinants of electrical rectification of single channel conductance in gap junctions formed by connexins 26 and 32. *J. Gen. Physiol.* 114:339–364.
38. Bukauskas, F. F., A. Bukauskiene, and V. K. Verselis. 2002. Conductance and permeability of the residual state of connexin43 gap junction channels. *J. Gen. Physiol.* 119:171–186.
39. Abrams, C. K., M. M. Freidin, V. K. Verselis, T. A. Bargiello, D. P. Kelsell, G. Richard, M. V. L. Bennett, and F. F. Bukauskas. 2006. Properties of human connexin 31, which is implicated in hereditary dermatological disease and deafness. *Proc. Natl. Acad. Sci. USA.* 103:5213–5218.
40. Bukauskas, F. F., A. Bukauskiene, M. V. Bennett, and V. K. Verselis. 2001. Gating properties of gap junction channels assembled from connexin43 and connexin43 fused with green fluorescent protein. *Biophys. J.* 81:137–152.
41. Meyer, R. A., D. W. Laird, J. P. Revel, and R. G. Johnson. 1992. Inhibition of gap junction and adherens junction assembly by connexin and A-CAM antibodies. *J. Cell Biol.* 119:179–189.
42. Moreno, A. P., J. G. Laing, E. C. Beyer, and D. C. Spray. 1995. Properties of gap junction channels formed of connexin 45 endogenously expressed in human hepatoma (SKHep1) cells. *Am. J. Physiol.* 268:C356–C365.

43. Bukauskas, F. F., C. Elfgang, K. Willecke, and R. Weingart. 1995. Biophysical properties of gap junction channels formed by mouse connexin40 in induced pairs of transfected human HeLa cells. *Biophys. J.* 68:2289–2298.

44. Hayrapetyan, V., and A. P. Moreno. 2003. Gating of heterotypic connexin40 and connexin45 gap junction channels. *Biophys. J.* 47: 5263a. (Abstr.)

45. Martinez, A. D., V. Hayrapetyan, A. P. Moreno, and E. C. Beyer. 2002. Connexin43 and connexin45 form heteromeric gap junction channels in which individual components determine permeability and regulation. *Circ. Res.* 90:1100–1107.

46. Valiunas, V., J. Gemel, P. R. Brink, and E. C. Beyer. 2001. Gap junction channels formed by coexpressed connexin40 and connexin43. *Am. J. Physiol. Heart Circ. Physiol.* 281:H1675–H1689.

47. Cottrell, G. T., Y. Wu, and J. M. Burt. 2002. Cx40 and Cx43 expression ratio influences heteromeric/ heterotypic gap junction channel properties. *Am. J. Physiol.* 282:C1469–C1482.

48. Lo, C. W. 2000. Role of gap junctions in cardiac conduction and development: insights from the connexin knockout mice. *Circ. Res.* 87:346–348.

49. Neijssen, J., C. Herberts, J. W. Drijfhout, E. Reits, L. Janssen, and J. Neefjes. 2005. Cross-presentation by intercellular peptide transfer through gap junctions. *Nature.* 434:83–88.

50. Valiunas, V., Y. Y. Polosina, H. Miller, I. A. Potapova, L. Valiuniene, S. Doronin, R. T. Mathias, R. B. Robinson, M. R. Rosen, I. S. Cohen, and P. R. Brink. 2005. Connexin-specific cell-to-cell transfer of short interfering RNA by gap junctions. *J. Physiol.* 568:459–468.

51. Mendez, C., W. J. Mueller, J. Merideth, and G. K. Moe. 1969. Interaction of transmembrane potentials in canine Purkinje fibers and at Purkinje fiber-muscle junctions. *Circ. Res.* 24:361–372.

52. Bukauskas, F. F., M. E. Sakson, and N. I. Kukushkin. 1976. Discrete zones of electrical connection between Purkinje terminals and muscle fibers in dog ventricles. *Biofizika.* 21:887–892.

53. Elfgang, C., R. Eckert, H. Lichtenberg-Frate, A. Butterweck, O. Traub, R. A. Klein, D. F. Hulser, and K. Willecke. 1995. Specific permeability and selective formation of gap junction channels in connexin-transfected HeLa cells. *J. Cell Biol.* 129:805–817.

54. Bennett, M. V., L. C. Barrio, T. A. Bargiello, D. C. Spray, E. Hertzberg, and J. C. Saez. 1991. Gap junctions: new tools, new answers, new questions. *Neuron.* 6:305–320.

55. Harris, A. L., and C. G. Bevans. 2001. Exploring hemichannel permeability in vitro. *Methods Mol. Biol.* 154:357–377.

56. Bukauskas, F. F., and V. K. Verselis. 2004. Gap junction channel gating. *Biochim. Biophys. Acta.* 1662:42–60.

57. Weingart, R., and F. F. Bukauskas. 1993. Gap junction channels of insects exhibit a residual conductance. *Pflugers Arch.* 424:192–194.

58. Moreno, A. P., M. B. Rook, G. I. Fishman, and D. C. Spray. 1994. Gap junction channels: distinct voltage-sensitive and - insensitive conductance states. *Biophys. J.* 67:113–119.

59. Verselis, V. K., C. S. Ginter, and T. A. Bargiello. 1994. Opposite voltage gating polarities of two closely related connexins. *Nature.* 368:348–351.

60. Ri, Y., J. A. Ballesteros, C. K. Abrams, S. Oh, V. K. Verselis, H. Weinstein, and T. A. Bargiello. 1999. The role of a conserved proline residue in mediating conformational changes associated with voltage gating of Cx32 gap junctions. *Biophys. J.* 76:2887–2898.

61. Martin, P. E., C. H. George, C. Castro, J. M. Kendall, J. Capel, A. K. Campbell, A. Revilla, L. C. Barrio, and W. H. Evans. 1998. Assembly of chimeric connexin-aequorin proteins into functional gap junction channels. Reporting intracellular and plasma membrane calcium environments. *J. Biol. Chem.* 273:1719–1726.

62. Bukauskas, F. F., K. Jordan, A. Bukauskiene, M. V. Bennett, P. D. Lampe, D. W. Laird, and V. K. Verselis. 2000. Clustering of connexin 43-enhanced green fluorescent protein gap junction channels and functional coupling in living cells. *Proc. Natl. Acad. Sci. USA.* 97:2556–2561.

63. Chen-Izu, Y., A. P. Moreno, and R. A. Spangler. 2001. Opposing gates model for voltage gating of gap junction channels. *Am. J. Physiol. Cell Physiol.* 281:C1604–C1613.

64. Hennemann, H., T. Suchyna, H. Lichtenberg Frate, S. Jungbluth, E. Dahl, J. Schwarz, B. J. Nicholson, and K. Willecke. 1992. Molecular cloning and functional expression of mouse connexin40, a second gap junction gene preferentially expressed in lung. *J. Cell Biol.* 117:1299–1310.

65. Kumari, S. S., K. Varadaraj, V. Valiunas, S. V. Ramanan, E. A. Christensen, E. C. Beyer, and P. R. Brink. 2000. Functional expression and biophysical properties of polymorphic variants of the human gap junction protein connexin37. *Biochem. Biophys. Res. Commun.* 274: 216–224.

66. Verselis, V. K., and F. F. Bukauskas. 2002. Connexin-GFPs shed light on regulation of cell-cell communication by gap junctions. *Curr. Drug Targets.* 3:483–499.

67. Auerbach, A. A., and M. V. L. Bennett. 1969. A rectifying electrotonic synapse in the central nervous system of a vertebrate. *J. Gen. Physiol.* 53:211–237.

68. Jaslove, S. W., and P. R. Brink. 1986. The mechanism of rectification at the electrotonic motor giant synapse of the crayfish. *Nature.* 323:63–65.

69. Giaume, C., R. T. Kado, and H. Korn. 1987. Voltage-clamp analysis of a crayfish rectifying synapse. *J. Physiol.* 386:91–112.

70. Giaume, C., and H. Korn. 1983. Bidirectional transmission at the rectifying electrotonic synapse: a voltage-dependent process. *Science.* 220:84–87.

71. Ramon, F., and A. Rivera. 1986. Gap junction channel modulation–a physiological viewpoint. *Prog. Biophys. Mol. Biol.* 48:127–153.

72. Chang, Q., A. Pereda, M. J. Pinter, and R. J. Balice-Gordon. 2000. Nerve injury induces gap junctional coupling among axotomized adult motor neurons. *J. Neurosci.* 20:674–684.

73. Guldenagel, M., G. Sohl, A. Plum, O. Traub, B. Teubner, R. Weiler, and K. Willecke. 2000. Expression patterns of connexin genes in mouse retina. *J. Comp. Neurol.* 425:193–201.